Optimal percolation of disordered segregated composites

Niklaus Johner,[*] Claudio Grimaldi,[†] Thomas Maeder, and Peter Ryser

LPM, Ecole Polytechnique Fédérale de Lausanne, Station 17, CH-1015 Lausanne, Switzerland
(Received 17 October 2008; revised manuscript received 19 December 2008; published 24 February 2009)

We evaluate the percolation threshold values for a realistic model of continuum segregated systems, where random spherical inclusions forbid the percolating objects, modeled by hardcore spherical particles surrounded by penetrable shells, to occupy large regions inside the composite. We find that the percolation threshold is generally a nonmonotonous function of segregation, and that an optimal (i.e., minimum) critical concentration exists well before maximum segregation is reached. We interpret this feature as originating from a competition between reduced available volume effects and enhanced concentrations needed to ensure percolation in the highly segregated regime. The relevance with existing segregated materials is discussed.

The percolation threshold of a two-phase heterogeneous system denotes the critical concentration at which global (long-range) connectivity of one phase is first established, and is accompanied by a sudden transition of the effective properties of the whole system [1,2]. Unlike the universal (or quasiuniversal) behavior of the critical exponents characterizing the percolative transition, the value of the percolation threshold is a function of several variables such as the shape of the percolating objects, their orientation and size dispersion, their possible interactions, and the microstructure in general [3].

Of fundamental importance for several technological applications is the possibility of exploiting such a multivariable dependence to lower the percolation threshold, so to have long-range connectivity of the percolating phase with the minimum possible critical concentration. This is the case when, for objects dispersed in a continuous medium, one wishes to exploit the properties of the percolating elements, but still preserving those of the host medium. For example, low conducting filler amounts in a conductor-insulator composite permit one to obtain an adequate level of electrical conductivity with mechanical properties of the composite being basically unaltered with respect to those of the pristine insulating phase.

In addition to the percolation threshold lowering driven by the large excluded volume of fillers with large aspect ratios such as rods and/or disks [4], the critical concentration can also be lowered by forbidding the percolating objects to occupy large (compared to the particle size) volumes inside the material, thereby leading to a segregated spatial distribution of the percolating phase. In practice, this can be achieved when elements of two (mutually impenetrable) species have different sizes and percolation is established by the smaller elements. Particle-laden foams [5], filled asphaltene matrices [6], and transport of macromolecules through porous media [7] are just a few cases where segregation governs the microstructure. However, the most typical examples of segregated systems are conductor-insulator composites having conducting particle sizes much smaller than those of

the insulating regions [8–10]. These materials display critical concentrations of a few percent or lower, which can be tuned by the degree of segregation in the system.

From the theoretical standpoint, segregated percolating composites represent an interesting class of interacting systems with an inhomogeneity length scale extending well beyond the characteristic size of the percolating objects. This must be contrasted to classical interacting systems such as hardcore, permeable, or sticking spheres models [3] where morphological inhomogeneities are set by the percolating particle sizes. However, despite the potential interest for both application and fundamental research, very few results exist on segregated percolation in the continuum [11], while the vast majority of studies is limited to lattice representations of the segregated structure [9,12], providing only a partial understanding of the percolation properties of segregated systems.

In this paper we consider a realistic continuum model of segregated percolation, primarily aimed at describing the microstructure of segregated conductor-insulator composites, but general enough to represent also other structurally similar systems. We show that, by varying the degree of segregation of the system, the percolation threshold is generally not a monotonous decreasing function of segregation, as suggested by earlier studies [9,11,12], but rather it displays a minimum before maximum segregation is reached. Hence, the optimal percolation threshold does not necessarily coincide with the most segregated structure, leading to a more complex phenomenology than previously thought.

We model a continuum segregated composite as schematically shown in Fig. 1(a). Namely, we consider one kind of impenetrable spherical particles of diameter d_1, which may refer to the conducting objects in a conductor-insulator composite, and a second kind of (insulating) spherical particles with diameter $d_2 \geq d_1$, which we allow to penetrate each other. Furthermore, to generate segregation, we assume that the two species of particles are mutually impenetrable, and that the voids left over from the two kinds of particles are filled by the second (i.e., insulating) phase. Finally, the connectivity criterion for the conducting phase is defined by introducing a penetrable shell of thickness $\delta/2$ surrounding each conducting sphere, so that two given particles are connected if their penetrable shells overlap. This model represents a rather faithful description of real segregated compos-

*niklaus.johner@epfl.ch
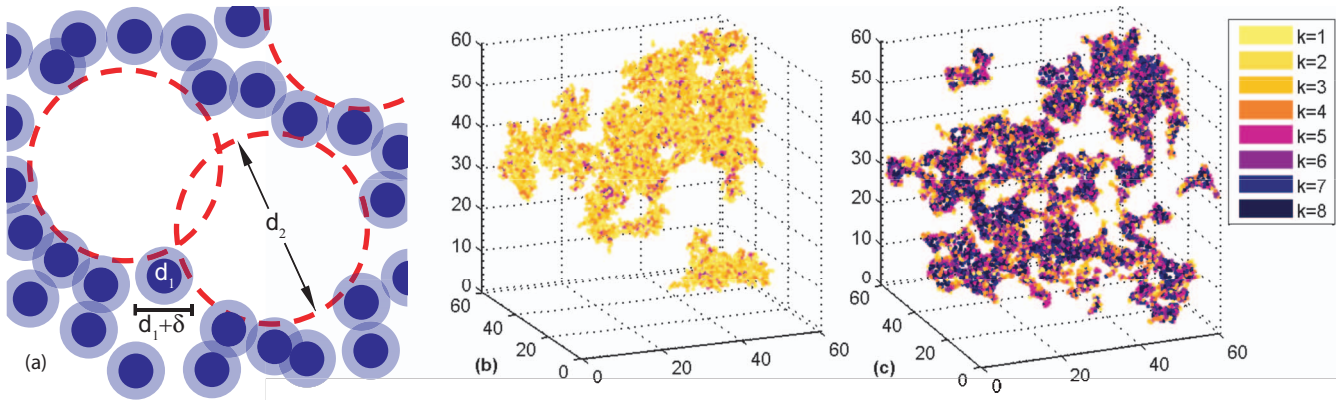†claudio.grimaldi@epfl.ch

FIG. 1. (Color) (a) Two-dimensional representation of the segregation model. The insulating spheres are represented by dashed circles, while the conducting particles are depicted by filled circles. (b) Percolating cluster of the conducting phase for the homogeneous case $\phi_2=0$ and (c) for the segregated regime with $d_2/d_1=12$ and $\phi_2=0.89$. The conducting particles are plotted together with their penetrable shells with $\delta=d_1$. The color map defines the values of the connectivity number k for each particle (see text).

ites, such as the RuO$_2$-glass systems [9,10], where thermal treatments on mixtures of RuO$_2$ and glassy grains lead to composites made of conducting RuO$_2$ particles dispersed in an insulating continuum. Segregation is induced by the larger size of the original glassy grains compared to that of the conducting particles. In the model, the insulating spheres are treated as overlapping to simulate glass melting and sintering during the firing process. Furthermore, in this and other similar classes of composites, electrical transport is given by direct tunneling or hopping processes, defining a characteristic length, represented by δ in our model, below which two conducting particles are electrically connected.

In our numerical simulations, the system described above is generated by first placing randomly the insulating spheres in a cube of edge length L with a given number density $\rho_2=N_2/L^3$, where N_2 is the number of spheres. The corresponding volume fraction for $L\rightarrow\infty$ is $\phi_2=1-\exp(-v_2\rho_2)$, where $v_2=\pi d_2^3/6$ is the volume of a single insulating sphere [3]. In a second step, N_1 conducting (and impenetrable) particles of diameter d_1 and number density $\rho_1=N_1/L^3$ are added in the remaining void space and a Metropolis algorithm is used to attain equilibrium [3]. In the following, for the conducting phase, we shall use the reduced concentration variable $\eta_1=\rho_1\pi(d_1+\delta)^3/6$.

In the absence of insulating spheres ($\phi_2=0$) the system so generated coincides with the semipenetrable spheres model [3,13,14], where the conducting particles are dispersed homogenously through the entire volume. On the contrary, for $\phi_2\neq 0$ the available volume fraction ϕ_{avail} for arranging the conducting particles gets lowered by the presence of the insulating spheres. By noticing that $\phi_{\mathrm{avail}}=\exp(-v_{\mathrm{excl}}\rho_2)$, where $v_{\mathrm{excl}}=\pi(d_2+d_1)^3/6$ is the excluded volume of an insulating sphere, and by using the definition of ϕ_2 given above, the available volume fraction is found to be

$$\phi_{\mathrm{avail}} = (1-\phi_2)^{(1+d_1/d_2)^3}, \tag{1}$$

which rapidly decreases as ϕ_2 and/or d_2/d_1 increase, so that a corresponding lowering of the critical density η_1^c is expected in this case.

Let us now assess the above available volume argument by a quantitative evaluation of the percolation threshold. For given values of d_2/d_1, δ, and ρ_2, and by using a modified Hoshen-Kopelman algorithm [15], we calculate as a function of η_1 and L the probability $P(\eta_1,L)$ that a cluster of phase 1 spans the system in a given direction, with periodic boundary conditions in the other two directions. The critical density $\eta_1^c(L)$ for finite L is then extracted from the condition $P(\eta_1,L)=1/2$ [16]. Examples of the resulting percolating clusters of the conducting phase for $L=60$ are shown in Fig. 1(b) for the homogeneous case ($\phi_2=0$) and in Fig. 1(c) for a segregated one with $d_2/d_1=12$ and $\phi_2=0.89$.

To obtain the critical density η_1^c for $L\rightarrow\infty$ we use the scaling relation $\eta_1^c(L)-\eta_1^c\propto L^{-1/\nu}$, where ν is the correlation length exponent obtained from the width of the transition. We considered eight different system sizes ranging from $L=16$ with $N_s=1500$ realizations to $L=60$ ($N_s=100$) for $d_2/d_1=1$ and from $L=60$ ($N_s=200$) to $L=140$ ($N_s=100$) for $d_2/d_1=12$. Twenty values of η_1 were typically used to fit $P(\eta_1,L)$ with an appropriate function. In this way, for most of the cases studied, the calculated ν values were well within 5% of the universal value $\nu\simeq 0.88$ [1].

Typical spanning probability results are reported in Fig. 2, where we plot $P(\eta_1,L)$ for $d_2/d_1=4$, $\delta=d_1$, and for two values of ϕ_2 with few different system sizes. Compared to the homogeneous case $\phi_2=0$, the spanning probability transition for $\phi_2\neq 0$ gets shifted to lower values of η_1, indicating that the percolation threshold is reduced by segregation. This is confirmed by the scaling analysis described above, which gives $\eta_1^c=0.3203\pm 0.0003$ for $\phi_2=0$, which is in very good accord with Refs. [13,14], and $\eta_1^c=0.1821\pm 0.0004$ for $\phi_2=0.65$.

Although the reduction of η_1^c shown in Fig. 2 has to be expected on the basis of reduced available volume argument given above, we find that, actually, η_1^c is generally a nonmonotonous function of ϕ_2. This is shown in Fig. 3(a) where η_1^c is plotted as a function of ϕ_2 for $\delta=d_1$ and for several values of d_2/d_1, and in Fig. 3(b) where $d_2/d_1=4$ and δ is varied. For all cases studied, as a function of ϕ_2, the behavior of the percolation threshold is characterized by an initial linear decrease of η_1^c, followed by a minimum at a particular value of
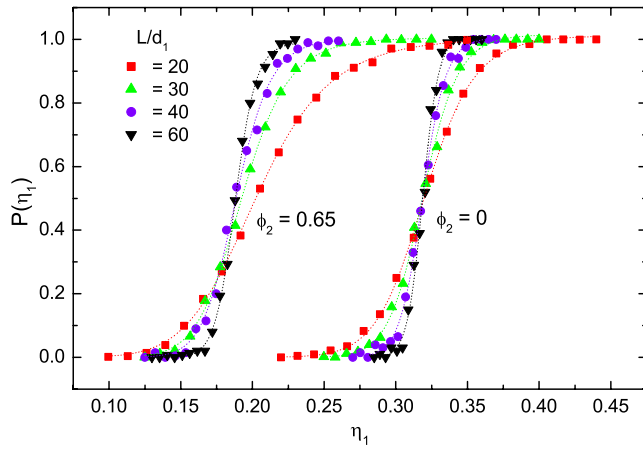
FIG. 2. (Color online) Spanning probability as a function of η_1 for a few values of the system linear size L and for two different values of insulating phase volume fraction ϕ_2. The penetrability length is $\delta=d_1$ and $d_2/d_1=4$.

FIG. 3. (Color online) Percolation threshold values η_1^c as a function of the volume fraction ϕ_2 of the insulating spheres for (a) $\delta=d_1$ and several values of d_2/d_1 and (b) $d_2/d_1=4$ and few values of δ. The vertical dashed lines are lower bounds of the maximum segregation obtained from Eq. (1), while the dotted lines are from Eq. (2).

ϕ_2 which depends upon d_2/d_1 and δ, and a final increase well before maximum segregation is reached at ϕ_2^*. Lower bounds of ϕ_2^* are plotted in Fig. 3 by vertical dashed lines, which are obtained by requiring that ϕ_{avail} [Eq. (1)] coincides with the percolating volume fraction of voids ϕ_{void}^c, which for the three dimensional penetrable sphere model used here is $\phi_{\text{void}}^c \simeq 0.03$ [17].

As shown in Fig. 3(a), the slope of the initial decrease of η_1^c is steeper for d_2/d_1 larger, and the position of the minimum gets shifted to higher values of ϕ_2. A similar effect is found by decreasing the penetrable shell thickness δ for fixed d_2/d_1, Fig. 3(b), leading to infer that for $\delta/d_2 \rightarrow 0$ the minimum disappears and η_1^c decreases monotonously all the way up to ϕ_2^*. These features, and in particular the appearance of a minimum (i.e., optimal) value of the percolation threshold for finite penetrable shells, represent our main finding and provide a previously unnoticed scenario for segregated percolation.

Let us discuss now the physical origin of the nonmonotonous behavior of the percolation threshold. The initial decrease of η_1^c can be fairly well reproduced by assuming that, for low values of ϕ_2, the volume fraction ϕ_1^c of the composite conducting particles (hardcore plus penetrable shell) is reduced by the volume occupied by insulating spheres. However, since the penetrable shells of the conducting particles may actually overlap the insulating spheres, these latter may be treated as having effectively a smaller volume $v_{\text{eff}} \leq v_2$, leading to $\phi_1^c(\phi_2) \simeq \phi_1^c(0)(1-\phi_2 v_{\text{eff}}/v_2)$. Taking into account that insulating particles with $d_2 \lesssim a$, where a is the mean distance between the closest surfaces of nearest neighbor conducting particles, should be ineffective in reducing ϕ_1^c, we approximate v_{eff} by a sphere of diameter d_2-a. Finally, by expanding $\phi_1^c(\phi_2)$ in powers of $\eta_1^c(\phi_2)-\eta_1^c(0)$, at the lowest order in ϕ_2 we find

$$\eta_1^c(\phi_2) \simeq \eta_1^c(0) - \frac{\phi_1^c(0)}{\phi_1^c(0)'}\left(\frac{d_2-a}{d_2}\right)^3 \phi_2, \quad (2)$$
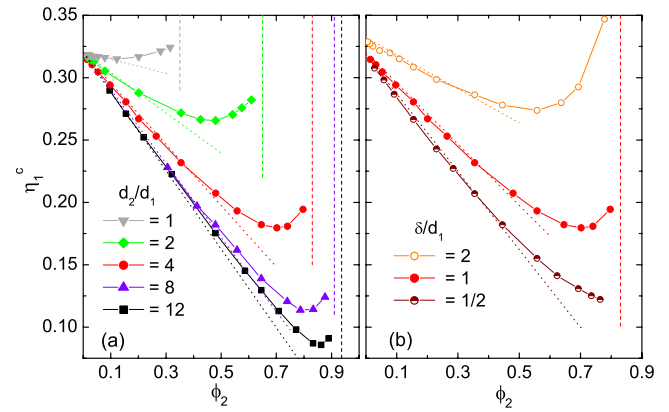
where $\phi_1^c(0)' = \lim_{\phi_2 \rightarrow 0} \delta\phi_1^c(\phi_2)/\delta\eta_1$. As it is seen in Fig. 3, where Eq. (2) (dotted lines) is plotted by using $a=(d_1+\delta)/2\,\eta_1^c(0)^{1/3}-d_1$ [14] and $\phi_1(0)$ as given in Ref. [3], the low ϕ_2 behavior of η_1^c is rather well reproduced for all cases considered.

By construction, the above argument neglects possible effects of $\phi_2 \neq 0$ on the connectivity number k, i.e., the number of conducting particles directly connected to a given one. Actually, as it is shown in Fig. 1 where the color map defines k for each particle in the percolating cluster, the rather narrow k distribution for the homogeneous case, which is peaked around the mean value $\langle k \rangle \simeq 2.25$ [13], changes drastically in the highly segregated regime of Fig. 1(c). Here, clusters of highly connected particles (k large) are bound together by "chains" of particles having low k values. Such distribution of k values is due to the fact that, in the vicinity of ϕ_2^*, the structure of the void space available for arranging the centers of the conducting particles is characterized by
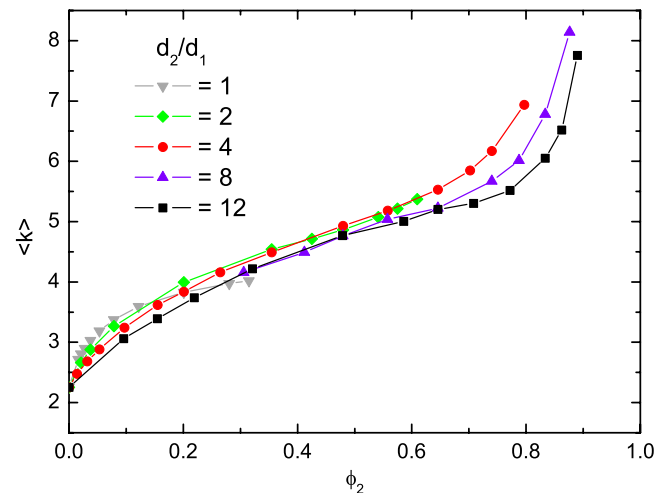

FIG. 4. (Color online) Mean connectivity number $\langle k \rangle$ as a function of ϕ_2 for the same cases of Fig. 3(a).

many narrow (quasi-one-dimensional) necks connecting more extended void regions [18]. Percolation is possible only if such necks are populated by connected conducting particles, and since for $\phi_2 \to \phi_2^*$ the necks become narrower, and so have less probability of being populated, more particles are needed to ensure connectivity, thereby "overcrowding" the many void regions between the necks. The net effect of such mechanism, not captured by Eq. (2), is the enhancement of η_1^c as $\phi_2 \to \phi_2^*$. This is demonstrated in Fig. 4 where $\langle k \rangle$, plotted for the same cases of Fig. 3(a), displays a sudden enhancement (more marked for d_2/d_1 larger) at values of ϕ_2 corresponding to the points of upturn of η_1^c of Fig. 3(a). The competition between the effect of reduced available volume, which lowers η_1^c [Eq. (2)], and the enhanced connectivity at high segregation, which increases η_1^c, is therefore at the origin of the minimum percolation threshold observed by us.

Before concluding, let us discuss the possibility of observing the features presented here in real segregated mate-rials. In conductor-insulator composites where transport is driven by tunneling, δ represents the maximum tunneling distance between the conducting particles, so that δ would be of the order of few nanometers. For such values of δ, the results of Fig. 3 would therefore apply to nanocomposites with $d_1 \approx \delta$ and d_2 not exceeding a few tens of nanometers. Much larger values of δ are, however, possible in some RuO_2-glass composites, where a reactive layer of thickness $0.2-0.4$ μm (or even more) surrounding the RuO_2 particles presents modified chemical and structural properties [19], most probably favoring hopping processes [20]. In this case, the parameters used in our work would easily account for composites with d_1 in the range $50-500$ nm and d_2 of few microns.

[1] D. Stauffer and A. Aharony, *Introduction to Percolation Theory* (Taylor & Francis, London, 1992).

[2] M. Sahimi, *Heterogeneous Materials I* (Springer, New York, 2003).

[3] S. Torquato, *Random Heterogeneous Materials: Microstructure and Macroscopic Properties* (Springer, New York, 2002).

[4] I. Balberg, C. H. Anderson, S. Alexander, and N. Wagner, Phys. Rev. B **30**, 3933 (1984); I. Balberg, *ibid.* **33**, 3618(R) (1986); E. Charlaix, J. Phys. A **19**, L533 (1986); I. Balberg and N. Binenbaum, Phys. Rev. A **35**, 5174 (1987); E. J. Garboczi, K. A. Snyder, J. F. Douglas, and M. F. Thorpe, Phys. Rev. E **52**, 819 (1995); T. Schilling, S. Jungblut, and M. A. Miller, Phys. Rev. Lett. **98**, 108303 (2007); G. Ambrosetti, N. Johner, C. Grimaldi, A. Danani, and P. Ryser, Phys. Rev. E **78**, 061126 (2008).

[5] S. Cohen-Addad, M. Krzan, R. Höhler, and B. Herzhaft, Phys. Rev. Lett. **99**, 168001 (2007).

[6] M. W. L. Wilbrink, M. A. J. Michels, W. P. Vellinga, and H. E. H. Meijer, Phys. Rev. E **71**, 031402 (2005).

[7] I. C. Kim and S. Torquato, J. Chem. Phys. **96**, 1498 (1992).

[8] R. Schueler, J. Petermann, K. Schute, and H.-P. Wentzel, J. Appl. Polym. Sci. **63**, 1741 (1997); W. J. Kim, M. Taya, K. Yamada, and N. Kamiya, J. Appl. Phys. **83**, 2593 (1998); C. Chiteme and D. S. McLachlan, Phys. Rev. B **67**, 024206 (2003).

[9] A. Kubovy, J. Phys. D **19**, 2171 (1986); A. Kusy, Physica B **240**, 226 (1997).

[10] P. F. Carcia, A. Ferretti, and A. Suna, J. Appl. Phys. **53**, 5282 (1982); S. Vionnet-Menot, C. Grimaldi, T. Maeder, S. Strässler, and P. Ryser, Phys. Rev. B **71**, 064201 (2005).

[11] A. S. Ioselevich and A. A. Kornyshev, Phys. Rev. E **65**, 021301 (2002); D. He and N. N. Ekere, J. Phys. D **37**, 1848 (2004).

[12] A. Malliaris and D. T. Turner, J. Appl. Phys. **42**, 614 (1971); R. P. Kusy, *ibid.* **48**, 5301 (1977); I. J. Youngs, J. Phys. D **36**, 738 (2003).

[13] D. M. Heyes, M. Cass, and A. C. Branca, Mol. Phys. **104**, 3137 (2006).

[14] N. Johner, C. Grimaldi, I. Balberg, and P. Ryser, Phys. Rev. B **77**, 174204 (2008).

[15] J. Hoshen and R. Kopelman, Phys. Rev. B **14**, 3438 (1976).

[16] R. M. Ziff, Phys. Rev. Lett. **69**, 2670 (1992); M. D. Rintoul and S. Torquato, J. Phys. A **30**, L585 (1997).

[17] J. Kertesz, J. Phys. (Paris), Lett. **42**, L393 (1981); W. T. Elam, A. R. Kerstein, and J. J. Rehr, Phys. Rev. Lett. **52**, 1516 (1984).

[18] S. Feng, B. I. Halperin, and P. N. Sen, Phys. Rev. B **35**, 197 (1987).

[19] K. Adachi, S. Iida, and K. Hayashy, J. Mater. Res. **9**, 1866 (1994).

[20] C. Meneghini, S. Mobilio, F. Pivetti, I. Selmi, M. Prudenziati, and B. Morten, J. Appl. Phys. **86**, 3590 (1999).